Performance study of a microfluidic reactor for cogeneration of chemicals and electricity

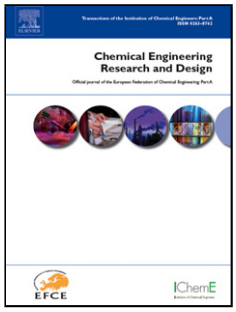

Title: Performance study of a microfluidic reactor for cogeneration of chemicals and electricity

Author: Benny Wouters Jonas Hereijgers Wim De Malsche Tom Breugelmans Annick Hubin

PII: S0263-8762(18)30649-X
DOI: https://doi.org/doi:10.1016/j.cherd.2018.12.023
Reference: CHERD 3471

To appear in:

Received date: 8 November 2018
Revised date: 19 December 2018
Accepted date: 22 December 2018

Please cite this article as: Benny Wouters, Jonas Hereijgers, Wim De Malsche, Tom Breugelmans, Annick Hubin, Performance study of a microfluidic reactor for cogeneration of chemicals and electricity, *<![CDATA[Chemical Engineering Research and Design]]>* (2018), https://doi.org/10.1016/j.cherd.2018.12.023

Performance study of a microfluidic reactor for cogeneration of chemicals and electricity

Benny Wouters[a,b,*], Jonas Hereijgers[b,c], Wim De Malsche[c], Tom Breugelmans[a,b], Annick Hubin[a]

[a] *Vrije Universiteit Brussel, Research Group Electrochemical and Surface Engineering, Pleinlaan 2, B-1050 Brussels, Belgium*
[b] *University of Antwerp, Research Group Advanced Reactor Technology, Universiteitsplein 1, B-2610 Wilrijk, Belgium*
[c] *Vrije Universiteit Brussel, Department of Chemical Engineering, Pleinlaan 2, B-1050 Brussels, Belgium*

Abstract

The chemical and electrochemical performance of a microfluidic reactor for the cogeneration of nitrobenzene derivatives and electricity has been analysed. Reactor operation has been tested using loads of 100Ω and 1000Ω, allowing an in-depth characterisation replicating the circumstances of actual chemical production. Conversion rates of up to 64% and power densities of up to 0.299mW cm^{-2} have been attained. The main products obtained using this cogeneration co-laminar flow cell (CLFC) are aniline and nitrosobenzene. Nitrosobenzene is identified as a product generated by cogeneration while aniline is established to be an unwanted side-product at the anode due to oxidant crossover, which reduces the cogeneration efficiency. Reactor stability has been determined by monitoring of the anode, cathode and cell potentials. Self-poisoning of the anode reaction leads to loss in electrical performance. Due to its ability to self-regenerate, the power density shows an oscillating behaviour over time. Results in this paper reveal that the concept of a cogeneration microreactor is promising, although the anode reaction and the mass transfer in the reactor can still be optimised further for actual applications.

Keywords: microfluidic reactor, co-laminar flow cell, electrochemical

*Corresponding author
Email address: benny.wouters@vub.be (Benny Wouters)

cogeneration, nitrobenzene, methanol oxidation

1. Introduction

The hydrogenation of nitrobenzene to aniline (AN) and phenylhydroxylamine (PHA) are typically performed in processes featuring highly exothermic reactions [1–4]. In most cases this heat cannot be transferred efficiently, leading to heat losses. Therefore, a more sustainable production pathway is searched for by both industry and academia. A possible solution is the cogeneration process in a fuel cell type reactor [5–7]. This process can be used in the case of thermodynamically spontaneous reactions. As opposed to other electrochemical production techniques, this electrochemical reactor uses chemical energy instead of electrical energy [6, 8]. This has the advantage that electrical energy can indeed be harvested from the system, instead of the system requiring electrical energy. The electricity produced can be regarded as energy savings. Compared to classical chemical hydrogenation of nitrobenzene, there are many additional benefits, including lower reactor temperatures and easier control of reactor selectivity [6]. Furthermore, expensive hydrogen is not required to supply this chemical energy. Lower-value chemicals such as methanol [9, 10] and formic acid [11, 12] can be used instead.

The electrochemical reduction mechanism of nitrobenzene leads to a range of useful chemicals [13–16], some of which are hard to obtain using conventional nitrobenzene reduction, e.g. azoxybenzene (AOB) is produced chemically using AN oxidation [17, 18], while the electrochemical process provides a direct route. This versatility is due to the high degree of control over the selectivity of the reactions: in addition to the temperature, acidity and the type of electrocatalyst, the potential of the electrode can also be controlled [19]. Scheme 1 displays the reaction scheme of the nitrobenzene reduction and its possible side reactions [20, 21]. The complex reaction mechanism leads to various ways of producing nitrobenzene derivatives electrochemically.

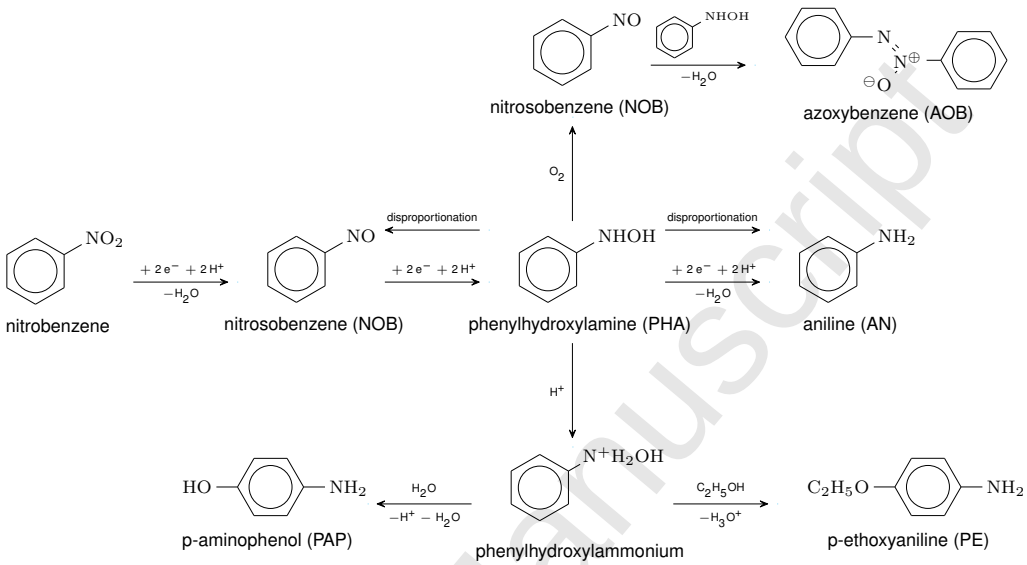

Scheme 1: Reaction scheme of the electroreduction of nitrobenzene in acidic ethanolic environment and possible side reactions.

In previously reported work [5] the cogeneration of nitrobenzene derivatives and electricity was performed in a PEM fuel cell reactor. In recent years, a lot of research has turned to electrochemical production in microfluidic reactors [22–25]. In this work, such a reactor based on the co-laminar flow cell (CLFC) design [26] is used for the cogeneration process. This design has several benefits, the most significant one being its membraneless design. As such, no new membranes need to be developed for this fuel cell design, which was reported as a subject requiring further research, specifically to increase proton conductivity [5].

In a previous paper [27] a preliminary study was performed to investigate the proof-of-concept for cogeneration in this reactor. While that has been established, the actual performance of the reactor under operating conditions is still unknown. This information can lead to new insights in terms of reactor optimisation. Therefore, the reactor performance during operation is assessed in this work. As before [27], the methanol oxidation and nitrobenzene reduction are taken as anodic and cathodic reactions, respectively. A copper-based catalyst capable of the selective reduction of nitrobenzene towards PHA [28] is used in

the reactor.

The performance of CLFCs is affected by a wide range of parameters, ranging from the electrocatalyst activity, the chosen reactions, mass transfer and ohmic losses [29]. The mass transfer rate is determined by the flow rate, fuel and oxidant concentration along with the cell and electrode geometry [30]. When operating the system as a fuel cell, the performance of a CLFC is usually a trade-off between power density and fuel utilisation [31]. However, for a cogeneration microreactor, it is more useful to look at the reactant conversion rather than at the fuel utilisation, although the same principles are still applicable.

To study the performance of the cogeneration microreactor, its spontaneous operation is examined over a prolonged period of time. Two different electrical loads, 1000Ω and 100Ω, are attached to the system to simulate actual production. The conversion and efficiency as a function of flow rate and load are examined. The load of 1000Ω is deemed to be closer to the electrical optimum, to optimise for maximal power output, while the load of 100Ω is closer to short-circuit conditions, optimising for maximal chemical conversion. The flow rate was set between 1 and 10µL min^{-1}.

The electrochemical behaviour during the cogeneration process was also analysed. The self-poisoning behaviour of the methanol oxidation, via the formation of adsorbed CO at the electrode surface, was identified as the cause behind the oscillating electrochemical behaviour of the reactor [27]. Its effect on the operation of the reactor is studied in this work by examining the stability in detail. For this purpose the cell, anode and cathode potentials have been monitored during the measurements.

2. Materials and methods

2.1. Materials

The catholyte employed during the measurements consisted of 0.025M nitrobenzene (Merck, 98%), dissolved in a 0.3M perchloric acid (VWR, Analar Normapur, 70%) solution in ethanol (VWR, Analar Normapur, 99.9%). The anolyte was a 0.1M methanol (VWR, Analar Normapur, 99.9%) dissolved in

1M aqueous sodium hydroxide (VWR, Analar Normapur, 99%) solution. The flow rate of these solutions was controlled using New Era NE-1000 and NE-1010 programmable syringe pumps.

2.2. Reactor construction

The construction of the CLFC has been detailed previously [27]. A top view of a 3D model of the bottom part of the CLFC is shown in figure 1. A y-shaped channel, consisting of two inlet channels and one main channel, was milled into a Delrin® polyoxymethylene (POM) part. The channel dimensions are 0.5x0.5x10mm for the inlet channels, and 1x0.5x30mm for the main channel. Graphite electrodes were used as walls of the main channel. An electrode surface area of 0.14cm^2 is available for both anode and cathode. The electrodes are coated with catalyst for a loading of 4.8µg mm^{-2}. As cathode catalyst, a copper nanoparticle catalyst supported on activated carbon has been employed [27, 28] and the anode catalyst is a commercial Pt-Ru nanoparticle catalyst supported on carbon black (Alfa Aesar®).

A rubber seal on top of the POM piece ensures a leak free construction.

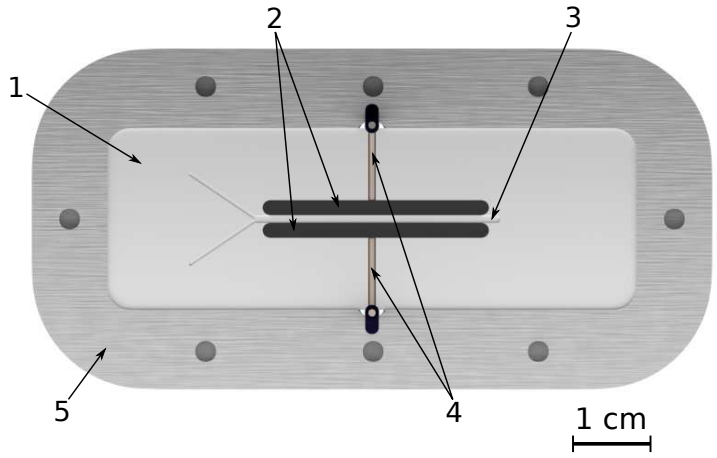

Figure 1: 2D view of the bottom part of the CLFC. (1) Machined polyoxymethylene (POM) piece; (2) graphite electrodes; (3) y-shaped channel formed by the machined POM and graphite electrodes; (4) electrical wires that are glued by silver epoxy to the graphite electrodes; (5) aluminium holder.

A Topas® cyclic olefin copolymer (COC) cover and a polymethylmethacrylate (PMMA) piece, wherein the nanoports for the tubing can be secured, cover the top. Two plates of aluminium were bolted together on both sides of the reactor to make sure all the pieces stay in place.

2.3. Electrochemical measurements

All electrochemical tests were done using a BioLogic VMP3 multichannel potentiostat. Two different loads, resistors of 100Ω and 1000Ω, were attached to the CLFC reactor. The loads enable power generation and production of useful chemicals. The measurement setup is depicted in figure 2. Measurements were performed at flow rates of 1, 2, 5 and 10µL min^{-1}. The flow rates mentioned in this paper are set for both the anolyte and the catholyte, so the flow rate in the main channel is actually twice the reported value. The solution at the exit of the CLFC was collected in a small recipient, containing 500µL of 0.3M solution of perchloric acid in ethanol and 500µL of 1M solution of sodium hydroxide and a reference electrode. A Ag/AgCl (sat. LiCl in ethanol, Autolab) electrode was placed in this solution, and this electrode is used for electrochemical monitoring during the measurement, and the initial solution provides the necessary conductivity. During all experiments, the cell, the anode and cathode potentials were measured separately using three different channels of the multichannel potentiostat.

2.4. UV-Vis spectrometry

UV-Vis detection was used to determine the concentration of the products formed. After the electrochemical measurement, three dilutions with a factor of 60 were made from the collected solution. These dilutions were measured individually using a HP 8452A UV-Vis spectrometer. The measured spectrum between 220 and 400nm was then fitted using known molar attenuation coefficients, calculated from calibration curves. The bootstrap [32] method with 1000 iterations was used to calculate the accuracy of the fit. After the fitting, the conversion and yields of the different products were calculated based on the different concentrations. The different possible products accounted for are nitrosobenzene

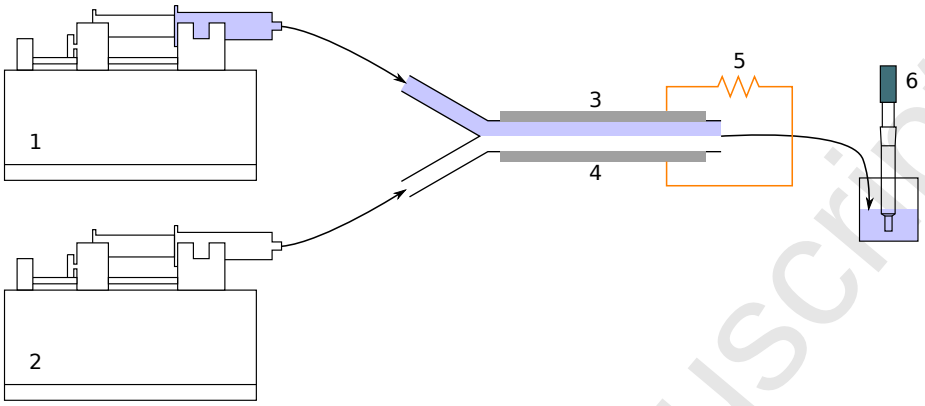

Figure 2: Schematic representation of the measurement setup. (1) Syringe pump controlling catholyte flow rate; (2) syringe pump controlling anolyte flow rate; (3) cathode; (4) anode; (5) electrical load; (6) reference electrode.

(NOB), PHA, AN, AOB, p-aminophenol (PAP) and p-ethoxyaniline (PE) (see Scheme 1).

3. Results and discussion

3.1. Electrochemical efficiency

3.1.1. Chemical performance

The chemical performance of the reactor is evaluated by the conversion of nitrobenzene, and the yield of the various reaction products. These quantities were determined by UV-Vis spectrometry. The results of this evaluation are shown in figure 3. Figure 3A shows that for a load of 1000Ω, the conversion of nitrobenzene varied between 37% and 64%. Interestingly, these values are much higher than the calculated theoretical conversion [27] of 11.7% at maximum power density and 26% at maximum current density. Increasing the flow rate decreased the conversion, although a plateau of around 40% was reached for flow rates between 2 and 10µL min^{-1}. The main reaction products were AN, NOB, and to a lesser extend PHA. Electrochemical testing of the catalyst [28] revealed that the cathode catalyst is selective towards PHA, making this a remarkable result. As PHA is unstable, it can be converted into different reaction products chemically (see Scheme 1), although the relative amount of AN is too high

to explain this discrepancy. This implies that AN is also produced through a different reaction. When the flow rate was increased in the reactor, the AN production was also increased at the expense of the NOB and PHA production. This indicates that mass transport is key to the reactions occurring at the electrodes.

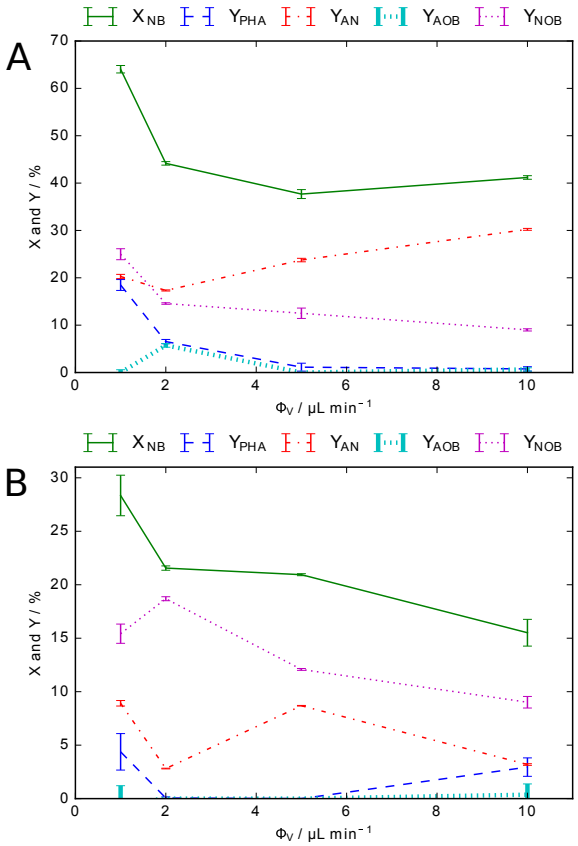

Figure 3: Chemical results of the cogeneration experiments. The conversion of nitrobenzene (X_{NB}) and yield of different products Y_a are displayed as a function of the flow rate Φ_V. The error bars represent the standard deviation of the sample mean. (A) load of 1000Ω; (B) load of 100Ω.

The results of the measurements with a load of 100Ω are depicted in figure 3B. This configuration is closer to short-circuit conditions, so higher conversions are expected. However, in this case the conversion was much lower than that observed with the load of 1000Ω. The values ranged from 14% to 28%, where the

highest value was again found at the lowest flow rate. While 2 and 5µL min^{-1} showed a similar conversion of around 20%, the conversion dropped to 14% at 10µL min^{-1}. The amount of NOB and PHA produced was similar to that with a load of 1000Ω, and it was also seen to be decreasing at higher flow rates. In contrast, the AN production was much lower, and no clear trend could be identified in its production.

3.1.2. Electrochemical performance

The overall electrochemical performance is studied by means of the average cell potentials. The results are shown in table 1. The values depicted in the table are the average cell potentials E_{cell}, the average current density j, the charge Q and the apparent Faraday efficiency η_{app}. The total charge required for conversion is obtained using Faraday's law, the concentrations of the different compounds, and the total volume of the solution, while the apparent Faraday efficiency is calculated by dividing this number by the total charge. The current density and total charge are not monitored, but instead they are calculated using Ohm's law and the value of the cell potential.

Table 1: Average electrochemical results of the cogeneration experiments. For each flow rate Φ_V, the average cell potential E_{cell}, the current and power densities (j and P), and the charge Q are shown as well as the apparent Faraday efficiency η_{app}, which is found by dividing the charge required to obtain the conversion of the products shown in figure 3 by Q.

Load (Ω)	Φ_V (µL min^{-1})	E_{cell} (V)	j (mA cm^{-2})	P (mW cm^{-2})	Q (C)	η_{app} (%)
1000	1	0.061	-0.433	0.0262	18.2	158
	2	0.078	-0.553	0.0430	11.6	172
	5	0.093	-0.665	0.0620	5.6	362
	10	0.205	-1.461	0.299	6.1	493
100	1	0.005	-0.310	$1.45{\cdot}10^{-3}$	11.2	86
	2	0.004	-0.245	$0.907{\cdot}10^{-3}$	5.5	121
	5	0.016	-1.065	0.0171	9.6	101
	10	0.020	-1.295	0.0257	5.8	88

For the results with a load of 1000Ω, the fact that the apparent Faraday efficiency of the experiments always surpassed 100% is immediately noticeable. It even reached a value of 493% at a flow rate of 10µL min^{-1}. This suggests that

the reduction of nitrobenzene at the cathode was not the only reaction occurring with nitrobenzene, as the charge provided to the cathode was insufficient for the measured conversion. Possible side reactions include fuel crossover, oxidant crossover, and chemical reactions taking place at the electrolyte interface. This matter will be investigated further in section 3.2.

The results with a load of 100Ω show a different trend, where the apparent Faraday efficiency exceeded 100% at 2 and 5µL min^{-1}, and was lower than 100% at 1 and 10µL min^{-1}. In the former case, the increase was much lower than that with the previous results. This means that the side reactions found with the measurements with a load of 1000Ω were less prominent in this system. The values of the apparent Faraday efficiency lower than 100% indicate a parasitic cathodic reaction, most likely to be oxygen reduction.

Looking at the electrical performance of the results with a load of 1000Ω, the power density steadily increased as the flow rate was increased, from 0.0262mW cm^{-2} at the lowest flow rate to 0.299mW cm^{-2} at the highest flow rate. This is a further indication that mass transport is key to the performance of the reactor. For optimised performance, the reactor at this electrical load should be run at a flow rate of 10µL min^{-1}.

From a power output perspective, the load of 100Ω is also not very favourable. The low cell potentials indicate near-short circuit conditions, resulting in low power densities especially at the low currents obtained at 1 and 2µL min^{-1}. The lowest average power output, at 2µL min^{-1}, is 0.907µW cm^{-2}, and the highest average power output is 0.0257mW cm^{-2} at 10µL min^{-1}. From the results with a load of 100Ω, it seems a flow rate of 5µL min^{-1} is the best combination of conversion and power.

3.2. Electrode reactions

3.2.1. Presence of side reactions

Because of the high apparent Faraday efficiency of the system, the presence of side reactions is expected in the reactor. Fuel and oxidant crossover provide a short circuit on the electrodes, and thus generate electrons that bypass the external circuit. Additionally, a chemical reaction occurring at the interface also

produces nitrobenzene derivatives without supplying electrons to the external circuit. As such, both could contribute to the high Faraday efficiency. To study whether any other chemical reactions take place in the cogeneration CLFC, a flow cell without electrodes was used in the same setup as the reactor. No products were formed using this setup, indicating that no chemical reactions take place between the different reagents.

Measurements without applying any external load were done to investigate the presence of oxidant and fuel crossover. As no electrons could transfer between the electrodes, the products formed in the reactor with these measurements are solely due to fuel and oxidant crossover (see figure 4). Products were formed in every measurement. The conversion of nitrobenzene was highest at a flow rate of $1\,\mu L\,min^{-1}$ at 18%. It was around 8 to 10% at higher flow rates. As before, NOB and AN were the main reaction products. For flow rates below $5\,\mu L\,min^{-1}$, the NOB and AN production was similar, whereas the AN production was again highest at $10\,\mu L\,min^{-1}$. It is possible that the reaction rate at the opposite electrode was slower for the experiments with a load, because the overpotential for the nitrobenzene reduction and methanol oxidation was lower. Nevertheless, these results still show a vast amount of fuel and/or oxidant crossover at all flow rates. This is consistent with the observations made in the electrochemical characterisation of this reactor [27].

3.2.2. Cogenerated and crossover products

Based on the chemical and electrochemical performance, there are some discrepancies in the data. The first one is the mixture of products formed: since the electrocatalyst is selective towards PHA [28], a mixture of nitrobenzene and PHA is expected, illustrated by figure 5. This is in contrast to the formed products, AN and NOB. Considering that the residence time in the reactor is high and PHA is very unstable, it is possible that PHA is indeed formed initially, but reacts away after a certain amount of time. As nitrobenzene is depleted on the cathode, AN might be formed due to the reduction of PHA. Another possible reaction is the decomposition of PHA into NOB and AN [33]. The PHA

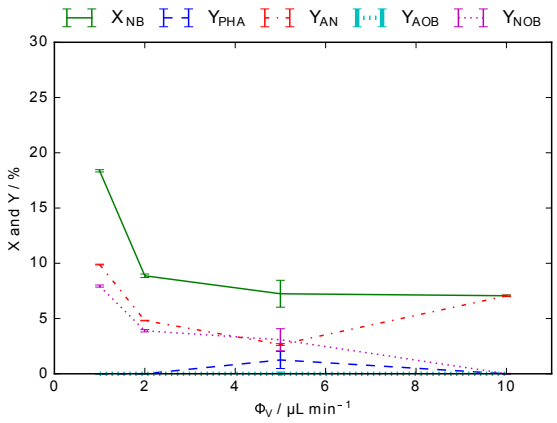

Figure 4: Chemical results of experiments with no load present. The conversion of nitrobenzene (X_{NB}) and yield of different products Y_a are displayed as a function of the flow rate Φ_V. The error bars represent the standard deviation of the sample mean.

might also be oxidised by oxygen towards NOB once the solution comes into contact with air at the exit of the reactor. Oxidant crossover might also have an influence on the selectivity as AN may be formed at the anode. While the conversion remains constant, the relative amount of AN also increases steadily as the flow rate increases. This might also be related to a decreasing pH as OH^- diffuses into the catholyte to a lesser extent.

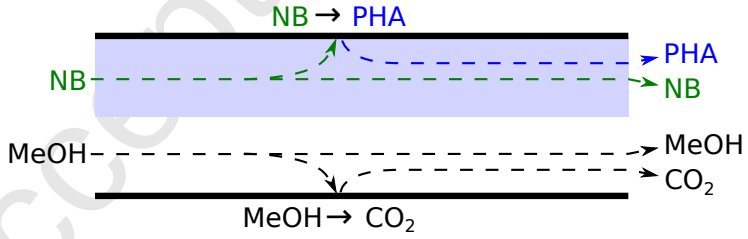

Figure 5: Expected cogeneration reactor behaviour, with nitrobenzene converting into PHA at the cathode. Methanol and CO_2 are indicated in black because they are not detected by the UV-Vis spectrometry.

The second discrepancy is the apparent efficiency exceeding 100%. As no chemical reactions occur between the reactants, this can only be explained by fuel and oxidant crossover. As oxidant reaches the anode, it finds a very high overpotential for its reduction, and thus converts instantly. This process

consumes current at the electrode that cannot be recorded by the electrochemical monitoring. However, this current is still used to reduce nitrobenzene at the anode, increasing the conversion. The same is true for fuel that reaches the cathode. As the apparent Faraday efficiency increases with the flow rate, the fuel and oxidant crossover also gain in relative importance compared to the cogeneration current. This could be related to the increasing relative amount of AN produced. If AN was produced separately at the anode through oxidant crossover, the remainder of the nitrobenzene derivatives produced would be related to PHA produced at the cathode. To investigate this hypothesis, the cogeneration efficiency η_c is calculated via equation 1, with n: number of moles, z: number of electrons transferred, F: Faraday constant.

$$\eta_c = \frac{Q_{\mathrm{PHA}}}{Q} = \frac{(n_{\mathrm{NOB}} + 2n_{\mathrm{AOB}} + n_{\mathrm{PHA}})z_{\mathrm{PHA}}F}{Q} \tag{1}$$

In this equation, the PHA related charge Q_{PHA} is compared with the measured charge Q. Q_{PHA} is calculated using Faraday's law and the amount of NOB, AOB and PHA. AOB is counted twice, as two PHA molecules are required to produce one molecule of AOB (Scheme 1). The results of this calculation are given in figure 6. As these values are always around 100%, this is an indication that AN is indeed produced electrochemically at the anode, due to oxidant crossover,

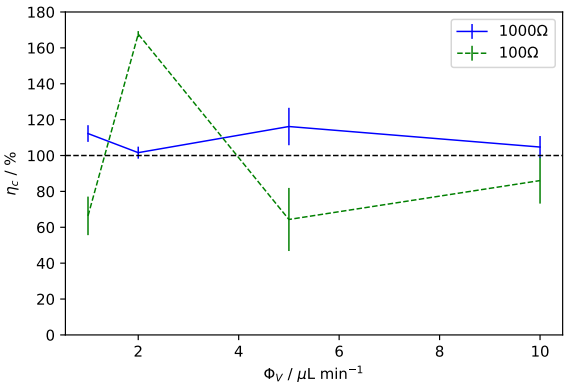

Figure 6: Cogeneration efficiency of the cogeneration experiments. The charge required to produce PHA-related products Q_{PHA} is compared to the measured charge Q as a function of the flow rate (equation 1).

while the other products are produced at the cathode, and they originate from PHA through chemical reactions (see Scheme 1). Figure 7 illustrates the actual behaviour of the reactor, with AN being produced at the anode because of oxidant crossover. The PHA formed at the cathode is later chemically oxidised to NOB.

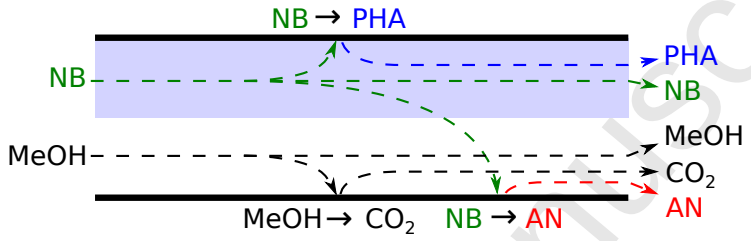

Figure 7: Actual cogeneration reactor behaviour, with nitrobenzene converting into PHA at the cathode and into AN at the anode.

For the results with a load of 1000Ω, the cogeneration efficiency was always slightly higher than 100%, indicating fuel crossover also played a role in the high efficiency. However, it only had a minor effect compared to the oxidant crossover. The values below 100%, obtained with a load of 100Ω, are proof that a parasitic reaction was also present in the system. This is most likely oxygen reduction, from the residual oxygen still present in the system. For the measurement with a flow rate of $2\,\mu L\,min^{-1}$, the high conversion efficiency could again be due to fuel crossover.

Comparing the results to the measurements with a load of 100Ω to those with a load of 1000Ω, nearly equal conversions are produced at flow rates of 5 and $10\,\mu L\,min^{-1}$ when only taking into account the products related to cogeneration. This is shown in figure 8. In this figure, the yields of all products related to PHA are summed up for each flow rate. The resulting graph shows the conversion related to cogeneration, X_c, exclusively. The cogenerated conversion is notably less at lower flow rates with a load of 100Ω. This is probably related to the low current densities measured at these flow rates, as seen in table 1.

With this information in mind the effects of the flow rate and the loading on the nitrobenzene production can be unravelled. As seen in the results, for

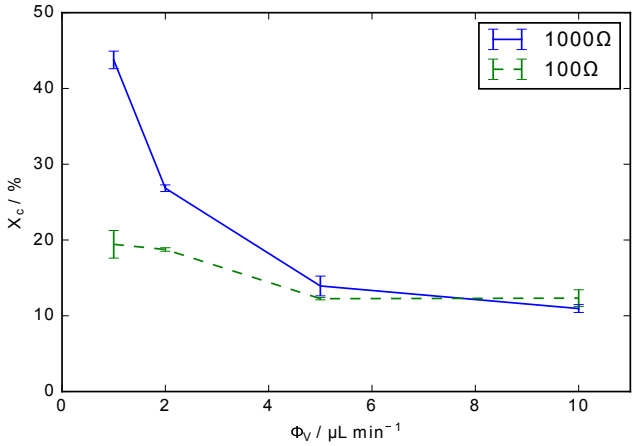

Figure 8: Comparison between the cogeneration-related conversion X_c as a function of the flow rate for the loads of 1000Ω and 100Ω.

a load of 1000Ω the relative amount of AN produced increases with the flow rate and the amount of cogenerated products decreases. The decrease of PHA-related conversion is an indication that the increased current is insufficient to compensate for the increased supply of nitrobenzene. The increased amount of AN is contrary to expectations, as less nitrobenzene crossover is expected. The logical conclusion is that the kinetics for the nitrobenzene reduction at the anode have increased.

The available electrochemically active surface area of the anode has a major influence on AN production. The presence of CO poisoning also interferes with this process and therefore, the increase in AN production found at higher flow rates is due to less self-poisoning behaviour of the anode, increasing the available surface area since it is not blocked by adsorbed CO. The irregular behaviour of the AN production at a load of 100Ω can be linked with varying degrees of CO poisoning.

3.2.3. Optimising the electrochemical performance

The electrode reactions seem to be mostly influenced by mass transfer phenomena, as fuel and oxidant crossover is the main factor influencing the products

formed. Lowering the fuel and oxidant crossover would mean an increase in selectivity of the reactor, as aniline would no longer be produced, and an increase in cogeneration conversion, as the parasitic reactions on the electrodes would be removed. Therefore, improving the mass transport in the reactor is key to optimisation. To solve the issues of fuel and oxidant crossover different channel designs such as an H-type channell [34] may be employed. Another approach would be to shorten the length of the channel to lower the diffusion time between the two electrolytes. This could be done in combination with the stacking of the devices [35]. If the shortening of the channel is done in the same manner as the indent this would not come at a cost of decreasing the electrode surface area. Another possible approach is to use hydrodynamic focusing [36], where a stream of electrolyte without any of the active components is introduced between the two electrolytes. This method could also increase nitrobenzene conversion rates.

3.3. Electrochemical stability

3.3.1. Electrochemical oscillations

The electrochemical performance of the reactor over time was studied by monitoring the electrode and cell potentials. In combination with the current density, calculated through Ohm's law, this provides information not only in terms of power generation but also in terms of electrochemical kinetics. The different experiments all showed a similar trend in terms of stability. For brevity, only one measurement is discussed in detail. The electrochemical performance over time of the measurement with a load of 100Ω and a flow rate Φ_V of 5µL min^{-1} is investigated. The results are displayed in figure 9A. In the upper graph, the cell potential and the current densities are shown. The graphs overlap since they are linearly related. The bottom graph in figure 9A shows the anodic and cathodic potentials individually during the measurement. It can clearly be seen in the plot that the cell potential, and therefore the power output, was not constant, but instead features oscillating behaviour. This oscillating behaviour is in line with potential oscillations due to CO poisoning found in literature [37–39].

Four distinct intervals could be identified per oscillation. These intervals are indicated in figure 9B, and are separated by dotted lines. To study the electrochemical oscillations in more detail, figure 9C provides a schematic representation of the anode and cathode potentials and current densities at the individual intervals. This figure will be used to clarify the explanations given below.

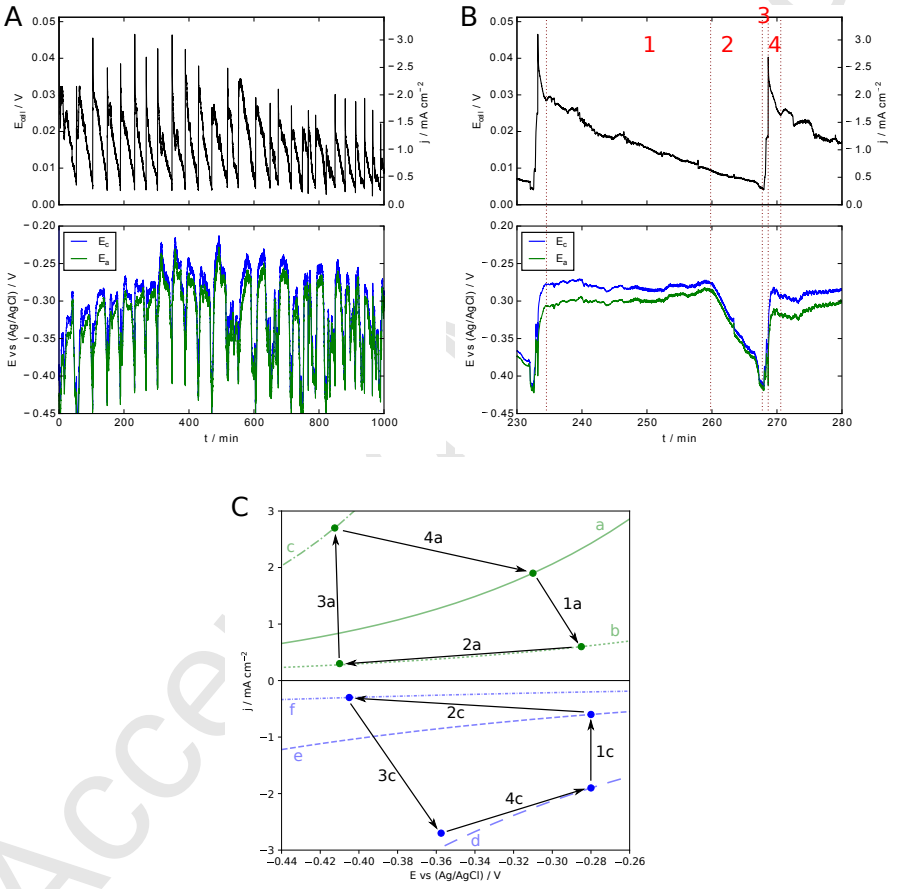

Figure 9: Electrochemical results obtained with a load of 100Ω and a flow rate of 5µL min^{-1}. The top graph depicts the cell potential (left hand axis) and current density (right hand axis). As the relationship between them is linear (Ohm's law) only one line is drawn for both quantities. The bottom graph shows the cathode (in blue) and anode potentials (in green). (A) complete measurement; (B) results between 230 and 280min. Different phases identified in the oscillating behaviour are indicated by numbers 1 to 4; (C) Schematic representation of the different electrochemical intervals during one period, as identified in (B). Possible anodic kinetics are indicated by letters a to c, possible cathodic kinetics are indicated by letters d to f.

The first interval was the longest one, and it was defined by the cell potential and current dropping steadily, while the cathode potential remains mostly stable and the anode potential increases slowly. The anode kinetics can be represented schematically by arrow 1a in figure 9C, where the kinetics drop from (a) to (b). This drop is related to CO poisoning on the anode. Interestingly, the cathode kinetics, represented by arrow 1c, also drop, from (d) to (e). The most likely explanation for this behaviour is fuel crossover as less methanol was oxidised at the cathode, leading to an increase in its concentration in the anolyte.

The second interval is marked by a large decline of both anode and cathode potentials while the current and cell potential drop at the same rate as in the first interval. Looking at figure 9C, mostly the cathodic kinetics drop tremendously, from (e) to (f). The great amount of fuel crossover, explained in interval 1, thus eventually lead to a collapse in cathode kinetics: the cathode potential had to decrease to keep up with the current of the anodic reaction.

The third interval has two parts in terms of the cell potential and current density: at first, it remained constant for approximately one minute, and then it increased to a peak. The anode and cathode potentials also remained constant for a while after which they both increased rapidly. This potential behaviour indicates a stabilisation and a breakthrough in the anodic and cathodic reactions. The stabilisation on the anodic side is due to to self-regeneration: as the surface gets completely covered with CO, the CO reduction becomes the major reaction and surface is liberated from CO. The surface thus becomes available again for the methanol reduction. This can be related to a galvanostatic oscillation, where the nitrobenzene acts as a constant source of electrons [38, 39] for the regeneration. As the anode starts reducing methanol again, fuel crossover is lowered. As a result, the apparent cathode kinetics increase, which provides the increase in current.

Interval 4 is marked by a rapid decrease in cell potential and current. Looking at figure 9C, mostly the anode kinetics were decreasing rapidly. In contrast to the first interval, the cathode kinetics remained stable. After interval 4, the cycle starts again at interval one, when the cathode kinetics start to be influenced by

the increased methanol concentration in the anolyte.

Comparing the anodic and cathodic potentials shown in figures 9A and B, it seems as if the behaviour shown in figure 9B is not representative for all other intervals, e.g. the plateau seems not to be present everywhere. However, after a closer inspection it was found that the behaviour is qualitatively the same, although the time scale of the different periods varies between intervals.

3.3.2. Catalyst layer degradation

As CO adsorption and subsequent regeneration is constantly occurring at the anode catalyst layer, its lifespan could be diminished. The influence of catalyst layer degradation is therefore studied next. For these experiments, the flow rate was set at $10\mu L\,min^{-1}$ and the load was 1000Ω. The experiment was repeated three times in series. Each experiment was run for 500 minutes. The results are show in figure 10. It can be seen that the nitrobenzene conversion drops from 41% to 14% after one measurement, indicating severe catalyst layer degradation. The relative amount of nitrosobenzene and aniline is also related to the catalyst layer age. In the first set of experiments, the amount of aniline surpasses that of nitrosobenzene, a trend that is reversed in the experiments performed at a later time. This is an indication that the anode kinetics for the nitrobenzene reduction decrease over time, most likely due to CO poisoning. The cogeneration conversion remains more stable, indicated by the NOB and PHA yields, although a slight decrease is observed.

As seen with the electrochemical oscillations, the deterioration of the anode catalyst could be reversible. The possibility of regeneration of the catalyst layer was tested by flushing it with electrolyte. The resulting data showed that the conversion of nitrobenzene increased to 25%, with a NOB yield of 10% and a AN yield of 15%, which is only a slight improvement over the third measurement in figure 10. Interestingly, both the AN yield and the NOB yield showed an increase. This again indicates the importance of crossed over methanol that does not react at the anode.

Because of the influence of catalyst layer degradation, the catalyst layer was

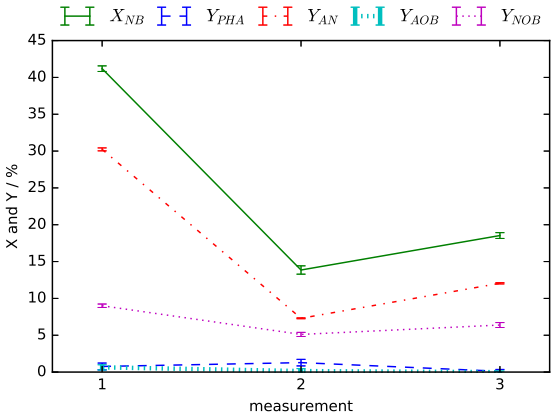

Figure 10: Chemical results of the catalyst degradation experiments with a flow rate of 10µL min^{-1}. The measurement was carried out with a load of 1000Ω. The conversion of nitrobenzene (X_{NB}) and yield of different products Y_a are displayed as a function of the flow rate.

regenerated between measurements by flushing it with electrolyte devoid of any active component. The catalyst layers were also replenished after a maximum of three measurements. The results with a load of 100Ω show that catalyst layer degradation could not be avoided completely: the amount of AN was highest at 5µL min^{-1}, which is chronologically the first measurement with this load. However, the studied trend is still clear so the measurements are reliable for this study.

3.3.3. Increasing the electrochemical stability

Overall, it can be stated that both the oscillating behaviour of the electrochemical performance and the degradation of the catalyst is mainly related to the self-poisoning nature of the anodic reaction. As a result, changing this reaction would increase the electrochemical stability of the reactor. A logical step is to look at reactions that do not have the rate-limiting step of adsorbed CO to CO_2 in their oxidation pathways. However, most organic fuels feature this step. A notable exception is the formic acid oxidation [40], which can form an active intermediate as well as a poison intermediate. The active intermediate is assumed to be adsorbed COOH [41], which already has two oxygen atoms attached to the carbon atom. In addition to this reaction, other possible fuels that do not exhibit

the self-poisoning reaction are non-organic fuels such as H_2O_2 [42, 43] and N_2H_4 [44], although these fuels could induce chemical side reactions happening between the fuel and oxidant, which would lower cogeneration efficiency.

4. Conclusions

The chemical and electrochemical performance of a microfluidic reactor for cogeneration of chemicals and electricity was studied. Both the influence of electrical load and flow rate was investigated. The hydrogenation of nitrobenzene was taken as a case study reaction. It was found that the reactor was capable of a conversion of 37% to 63% when paired with a load of 1000Ω, forming mostly nitrosobenzene and aniline. Phenylhydroxylamine was found to be the cogenerated product, and it was oxidised to nitrosobenzene by oxygen due to exposure to air. Aniline was identified as an unwanted side-product produced by crossed over oxidant at the anode. This means that although the overall conversion of the reactor was adequate, the actual cogeneration process was working much less efficiently. The cell potential and current density, and subsequently the power density, increased steadily as flow rate was increased indicating the influence of mass transfer. The cogeneration conversion of nitrobenzene decreased with higher flow rates.

The electrochemical performance of the reactor was unstable over time: the self-poisoning behaviour of the anode reaction led to oscillating power densities, similar to methanol oscillations during oxidation, as also seen in literature. Nitrobenzene acted as a constant source of electrons at the anode, which induced regeneration. In the oscillation cycles, not only the anode reaction was affected: due to the increased methanol concentration, fuel crossover was not constant, which resulted in oscillations in cathode kinetics as well.

Based on these results, the reactor performance can be increased through two separate pathways. Fuel and oxidant crossover is the first major issue identified in this reactor, especially due to the low flow rates required to reach optimal conversions. This could be dealt with by optimising the design of the flow channel. Secondly, a different anode reaction, that does not include the

adsorbed CO intermediate, would remove the oscillating behaviour found in the electrochemical stability measurements, and increase the lifespan of the catalyst layer.

Acknowledgements

The authors would like to thank Dr. Xia Sheng and Prof. Dr. Paolo P. Pescarmona from the University of Leuven (KU Leuven) for supplying the cathode electrocatalyst, Dr. Patrick Steegstra for his assistance in the lab, Prof. Dr. ir. Yves Rolain and Prof. Dr. ir. Rik Pintelon for their assistance with the statistical analysis of the data, and Priya Laha for proofreading the manuscript.

References

[1] G. R. Maxwell, Synthetic Nitrogen Products: A practical Guide to the Products and Processes, Kluwer Academic Publishers, 2004.

[2] H. H. Byung, H. S. Dae, Y. C. Sung, Graphite catalyzed reduction of aromatic and aliphatic nitro compounds with hydrazine hydrate, Tetrahedron Lett. 26 (50) (1985) 6233–6234.

[3] J. W. Larsen, M. Freund, K. Y. Kim, M. Sidovar, J. L. Stuart, Mechanism of the carbon catalyzed reduction of nitrobenzene by hydrazine, Carbon 38 (5) (2000) 655–661.

[4] P. N. Rylander, I. M. Karpenko, G. R. Pond, Process for preparing para-aminophenol, US Patent 3715397, 1973.

[5] X.-Z. Yuan, Z.-F. Ma, Q.-Z. Jiang, W.-S. Wu, Cogeneration of cyclohexylamine and electrical power using PEM fuel cell reactor, Electrochem. Commun. 3 (2001) 599.

[6] F. Alcaide, P.-L. Cabot, E. Brillas, Fuel cells for chemical and energy cogeneration, J. Power Sources 153 (2006) 17–60.

[7] Z. Pan, R. Chen, L. An, Y. Li, Alkaline anion exchange membrane fuel cells for cogeneration of electricity and valuable chemicals, J. Power Sources 365 (2017) 430–445.

[8] S. H. Langer, H. P. Landi, Electrogenerative Hydrogenation, J. Am. Chem. Soc. 85 (1963) 3043–3044.

[9] M. Watanabe, S. Motoo, Electrocatalysis by ad-atoms part II. Enhancement of the oxidation of methanol on platinum by ruthenium ad-atoms, Electroanal. Chem. 60 (1975) 267–273.

[10] S. Wasmus, A. Küver, Methanol oxidation and direct methanol fuel cells: a selective review, Electroanal. Chem. 461 (1999) 14–31.

[11] M. Weber, J. T. Wang, S. Wasmus, R. F. Savinell, Formic acid oxidation in a polymer electrolyte fuel cell - A real-time mass-spectrometry study, J. Electrochem. Soc. 143 (7) (1996) L158–L160.

[12] Y. Zhu, S. Y. Ha, R. I. Masel, High power density direct formic acid fuel cells, J. Power Sources 130 (2004) 8–14.

[13] J.-C. Gard, J. Lessard, Y. Mugnier, An efficient electrochemical method for the synthesis of nitrosobenzene from nitrobenzene, Electrochim. Acta 38 (5) (1993) 677–680.

[14] J. C. Smeltzer, P. S. Fedkiw, Reduction of Nitrobenzene in a Parallel-Plate Reactor I. Differential Conversion Using Periodic Cell-Voltage Control, J. Electrochem. Soc. 139 (5) (1992) 1358–1366.

[15] J. C. Smeltzer, P. S. Fedkiw, Reduction of Nitrobenzene in a Parallel-Plate Reactor II. Integral Conversion Using Periodic Cell-Voltage Control, J. Electrochem. Soc. 139 (5) (1992) 1366–1372.

[16] Y.-P. Sun, W.-L. Xu, K. Scott, A study of the electrochemical reduction of nitrobenzene to p-aminophenol in a packed-bed reactor, Electrochim. Acta 38 (13) (1993) 1753–1759.

[17] H. R. Sonawane, A. V. Pol, P. P. Moghe, S. S. Biswas, A. Sudalai, Selective catalytic oxidation of arylamines to azoxybenzenes with H2O2 over zeolites, J. Chem. Soc. Chem. Comm. 10 (1994) 1215–1216.

[18] Y. S. S. Wan, K. L. Yeung, A. Gavriilidis, TS-1 oxidation of aniline to azoxybenzene in a microstructured reactor, Appl. Catal. A: Gen. 281 (2005) 285–293.

[19] H. Rance, J. Coulson, The electrolytic preparation of p-aminophenol, Electrochim. Acta 14 (4) (1969) 283–292.

[20] J. Marquez, D. Pletcher, A study of the electrochemical reduction of nitrobenzene to p-aminophenol, J. Appl. Electrochem. 10 (1980) 567–573.

[21] H. Lund, Cathodic reduction of nitro and related compounds, in: Organic electrochemistry, Marcel Dekker New York, 4th edn., 379–409, 2001.

[22] M. Atobe, Organic electrosynthesis in flow microreactor, Curr. Opin. Electrochem. 2 (1) (2017) 1–6.

[23] M. Atobe, H. Tateno, Y. Matsumura, Applications of flow microreactors in electrosynthetic processes, Chem. Rev. 118 (9) (2018) 4541–4572.

[24] T. Hardwick, N. Ahmed, Advances in electro-and sono-microreactors for chemical synthesis, RSC Adv. 8 (39) (2018) 22233–22249.

[25] M. Islam, B. M. Kariuki, Z. Shafiq, T. Wirth, N. Ahmed, Efficient Electrosynthesis of Thiazolidin-2-imines via Oxysulfurization of Thiourea-Tethered Terminal Alkenes using the Flow Microreactor, Eur. J. Org. Chem. .

[26] R. Ferrigno, A. D. Stroock, T. D. Clark, M. Mayer, G. M. Whitesides, Membraneless Vanadium Redox Fuel Cell Using Laminar Flow, J. Am. Chem. Soc. 124 (2002) 12930–12931.

[27] B. Wouters, J. Hereijgers, W. De Malsche, T. Breugelmans, A. Hubin, Electrochemical characterisation of a microfluidic reactor for cogeneration of chemicals and electricity, Electrochim. Acta 210 (2016) 337–345.

[28] X. Sheng, B. Wouters, T. Breugelmans, A. Hubin, I. F. J. Vankelecom, P. P. Pescarmona, Pure and Alloyed Copper-Based Nanoparticles Supported on Activated Carbon: Synthesis and Electrocatalytic Application in the Reduction of Nitrobenzene, ChemElectroChem 1 (7) (2014) 1198–1210.

[29] S. A. M. Shaegh, N.-T. Nguyen, S. H. Chan, A review on membraneless laminar flow-based fuel cells, Int. J. Hydrogen Energy 36 (9) (2011) 5675–5694.

[30] M. N. Nasharudin, S. K. Kamarudin, U. A. Hasran, M. S. Masdar, Mass transfer and performance of membrane-less micro fuel cell: A review, Int. J. Hydrogen Energy 39 (2) (2014) 1039–1055.

[31] R. S. Jayashree, S. K. Yoon, F. R. Brushett, P. O. Lopez-Montesinos, D. Natarajan, L. J. Markoski, P. J. Kenis, On the performance of membraneless laminar flow-based fuel cells, J. Power Sources 195 (11) (2010) 3569–3578.

[32] B. Efron, R. J. Tibshirani, An Introduction to the Bootstrap, Chapman & Hall/CRC, 1998.

[33] D. Grošková, M. Štolcová, M. Hronec, Reaction of N-phenylhydroxylamine in the presence of clay catalysts, Catal. Lett. 69 (2000) 113–116.

[34] H. B. Park, D. H. Ahmed, K. H. Lee, H. J. Sung, An H-shaped design for membraneless micro fuel cells, Electrochim. Acta 54 (18) (2009) 4416–4425.

[35] K. S. Salloum, J. D. Posner, A membraneless microfluidic fuel cell stack, J. Power Sources 196 (2011) 1229–1234.

[36] J. Xuan, M. K. Leung, D. Y. Leung, M. Ni, H. Wang, Hydrodynamic focusing in microfluidic membraneless fuel cells: Breaking the trade-off between fuel utilization and current density, Int. J. Hydrogen Energy 36 (2011) 11075–11084.

[37] M. T. Koper, T. J. Schmidt, N. M. Marković, P. N. Ross, Potential oscillations and S-shaped polarization curve in the continuous electro-oxidation of CO on platinum single-crystal electrodes, J. Phys. Chem. B 105 (35) (2001) 8381–8386.

[38] G. Horanyi, Heterogeneous catalysis and electrocatalysis, Catal. Today 19 (2) (1994) 285–311.

[39] P. Strasser, M. Eiswirth, M. T. Koper, Mechanistic classification of electrochemical oscillators—an operational experimental strategy, J. Electroanal. Chem. 478 (1) (1999) 50–66.

[40] J. M. Feliu, E. Herrero, Formic acid oxidation, in: Handbook of Fuel Cells, John Wiley & Sons, Ltd, 1–10, 2010.

[41] S. Sun, J. Clavilier, A. Bewick, The mechanism of electrocatalytic oxidation of formic acid on Pt (100) and Pt (111) in sulphuric acid solution: an emirs study, J. Electroanal. Chem. 240 (1) (1988) 147–159.

[42] S. Hasegawa, K. Shimotani, K. Kishi, H. Watanabe, Electricity Generation from Decomposition of Hydrogen Peroxide, Electrochem. Solid St. 8 (2) (2005) A119–A121.

[43] E. Kjeang, A. G. Brolo, D. A. Harrington, N. Djilali, D. Sinton, Hydrogen peroxide as an oxidant for microfluidic fuel cells, J. Electrochem. Soc. 154 (12) (2007) B1220–B1226.

[44] R. Parsons, T. VanderNoot, The oxidation of small organic molecules: a survey of recent fuel cell related research, J. Electroanal. Chem. 257 (1) (1988) 9–45.

Research highlights

- The operation of a cogeneration microreactor for nitrobenzene reduction is studied
- Phenylhydroxylamine is identified as the main cogenerated reaction product
- Aniline is produced as a side product due to oxidant crossover
- The reactor selectivity can be increased by improving the flow channel design
- The stability can be increased by changing the anode reaction or the anode catalyst